A NONLINEAR INVERSION METHOD FOR DERIVATION OF TEMPERATURE PROFILES FROM TOVS-DATA

J. Svensson

The Swedish Meteorological and Hydrological Institute (SMHI)
Norrköping, Sweden

1. INTRODUCTION

The Physical Retrieval TOVS Export Package, developed by the Cooperative Institute for Meteorological Satellite Studies (CIMSS), Madison, Wisconsin, has been implemented on the computer system at SMHI. The ONSAM-experiment gave an opportunity to test the software package. The ONSAM-experiment took place at Onsala Space Observatory ($57^{o}24'$N, $11^{o}55'$E), May 2-26, 1983. The primary objective of this project was to test the performance and profiling capability of ground-based temperature and water vapour microwave radiometers developed at Chalmers University of Technology (Askne, 1984).

During the ONSAM-experiment TIP-data were received from the Danish Meteorological Institute, Observatory for Space Research, Rude Skov, Birkeröd, Denmark, where a read-out station is situated. The implementation of the TOVS Export Package and test results are described by Svensson (1984). The results from the TOVS Export Package are compared to those from a new physical, nonlinear inversion method developed at SMHI. In the development of the new inversion method the approach was

1) efficient and publically available numerical software should be used,
2) the method should be easy to analyse,
3) new ancillary data should be easy to incorporate.

Those readers who are not already familiar with the characteristics of the TIROS Operational Vertical Sounder (TOVS) are referred to Lauritsen et al (1979), Werbowetski (1981) or Smith and Woolf (1976).

2. INVERSION METHOD

The basis of the inversion method is the radiative transfer equation (RTE). Surface observations of temperature, humidity and pressure are also incorporated in the inversion method. Basis splines (B-splines) have been used to represent the temperature and humidity profiles. Some physical constraints, represented as linear inequality constraints are also included. This leads to a linear least-squares problem with linear inequality constraints to solve. Because of the nonlinear properties of the radiative transfer equation, we may have to repeat this process once or twice.

This chapter describes all the parts of the inversion method, which is called THAP (Temperature and Humidity Atmospheric Profiler). More details about the algorithms and computations are found in Svensson (1985).

2.1 Radiative transfer equation

The radiative transfer equation for satellite based radiance measurements is

$$\gamma_\nu = \varepsilon_\nu \cdot B_\nu(T_S) \cdot \tau_\nu(P_S) - \int_0^{P_S} B_\nu(T) \cdot \frac{\partial \tau_\nu(P)}{\partial P} \cdot dP,$$

where the following notation is used:

γ_ν	radiance measured at channel 'ν',
ν	channel number (20 infrared and 4 microwave channels are available),
P	pressure (P_S is surface pressure),
$T(P)$	temperature (T_S is surface skin temperature),
ε_ν	emissivity,
$\tau_\nu(P)$	transmittance,
$B_\nu(T)$	Planck function.

The dependency of zenith angle is to be understood. Calculation of transmittance is described in Weinreb et al (1981). These calculations are made available through a NOAA software package for 40 different levels, between 0.1 and 1000 mb. For simplicity we assume that P_S is 1000 mb. Transmittance depends not only on frequency, angle and pressure level, but also on temperature, water content and ozone content between the pressure level of interest and the satellite. We also define

$W(P)$	water vapour mixing ratio (g/kg),
$V(P)$	ln (W).

Throughout this paper, we will indicate matrices with a double wavy underline and vectors with one wavy underline. The element in row 'i' and column 'j' for a matrix $\underset{\approx}{A}$ is denoted a_{ij} and the element 'i' in a vector $\underset{\sim}{A}$ is denoted a_i. Especially we note that P, T and V are vectorized into $\underset{\sim}{P}$, $\underset{\sim}{T}$ and $\underset{\sim}{V}$ for the 40 pressure levels.

2.2 Taylor expansion

Suppose we have an initial guess of temperature, surface skin temperature and humidity ($T^{(0)}$, $T_S^{(0)}$ and $V^{(0)}$). We make a first-order Taylor expansion about $T^{(0)}$, $T_S^{(0)}$ and $V^{(0)}$ and get

$$y_\nu = \gamma_\nu - \varepsilon_\nu \cdot B_\nu(T_S^{(0)}) \cdot \tau_\nu(P_S) + \int_0^{P_S} B_\nu(T^{(0)}) \cdot \frac{\partial \tau_\nu(P)}{\partial P} \cdot dP$$

$$\approx \frac{\partial \gamma_\nu}{\partial \underset{\sim}{T}} \cdot \Delta \underset{\sim}{T} + \frac{\partial \gamma_\nu}{\partial T_S} \cdot \Delta T_S + \frac{\partial \gamma_\nu}{\partial \underset{\sim}{V}} \cdot \Delta \underset{\sim}{V}. \qquad (1)$$

In the calculation of the partial derivatives we use standard software for numerical differentiation and numerical quadrature. Equation (1) may in a shorter form be written

$$\underset{\sim}{Y} = \underset{\approx}{R}_T \cdot \Delta\underset{\sim}{T} + \underset{\sim}{R}_S \cdot \Delta T_S + \underset{\approx}{R}_V \cdot \Delta\underset{\sim}{V} ,$$

where $\underset{\approx}{R}_T$ and $\underset{\approx}{R}_V$ are mxn-dimensional matrices, $\underset{\sim}{R}_S$ is a m-dimensional vector, m is the number of frequencies and n is the number of pressure levels (=40). With $\underset{\sim}{T}^{(0)} + \Delta\underset{\sim}{T}$, $T_S^{(0)} + \Delta T_S$ and $\underset{\sim}{V}^{(0)} + \Delta\underset{\sim}{V}$, we receive better approximation of $\underset{\sim}{T}$, T_S and $\underset{\sim}{V}$.

In order to scale the equations properly, each equation, corresponding to channel ν should be multiplied by $1/\frac{\partial B_\nu(B_\nu^{-1}(\gamma_\nu))}{\partial T}$. The term $B_\nu^{-1}(\gamma_\nu)$ is called brightness temperature. The weights, of each equation, are based upon the estimated errors in the brightness temperature for each frequency.

2.3 Ancillary data

Ancillary data are given by surface observations of temperature (T_{OBS}) and humidity ($V_{OBS} = \ln(W_{OBS})$. This will give two equations

$$\Delta t_{40} = T_{OBS} - t_{40}^{(0)} \tag{2}$$

and

$$\Delta v_{40} = V_{OBS} - v_{40}^{(0)} . \tag{3}$$

The initial temperature profile is given for 40 levels. However we only allow ΔT to be non-zero for pressure levels up to 10 mb (which corresponds to level 11). Besides we require that Δt_{11} should not be too large. This will give the equation

$$\Delta t_{11} = 0 . \tag{4}$$

The difference between the variables t_{40} and T_S is assumed to be small. The equation

$$\Delta t_{40} - \Delta T_S = T_S^{(0)} - t_{40}^{(0)} \tag{5}$$

will express this relation.

The equations (2)-(5) are weighted, based upon the estimated errors in the variables involved.

2.4 B-splines

We use a set of basis functions, for the variables T and V, instead of discretizing the variables in 40 levels. This will increase the accuracy of the solution and decrease the number of arithmetic operations. We choose cubic B-splines, with ln(P) as independent variable, to form the basis functions. Some very attractive features of B-splines are

1) well-developed theory,
2) excellent approximation properties; the function, its integral and derivatives are calculated easy and accurate,
3) publically available numerical software exists.

B-splines are described by de Boor (1978).

We have already mentioned, that we do not allow the temperature to be changed above the 10 mb-level. Besides we do not allow the water vapour to be changed over the 300 mb-level (level 26). This can be expressed in the choice of the knots, which define the B-splines. The knots for the B-splines representing T are the logarithms of $\Psi_T = \{4{*}10, 100,200,300,400,500,600,700,850,4{*}1000\}$.

Thus we may express the initial guess temperature profile up to 10 mb as

$$T^{(0)}(P) = \sum_{i=1}^{12} c_i \cdot B_i(\Psi_T, P) \quad ,$$

where c_i are spline coefficients for temperature profile and $B_i(\Psi_T,P)$ is the B-spline 'i' for the given set of knots, Ψ_T, at pressure P.

In the same way we will have

$$V^{(0)}(P) = \sum_{i=1}^{9} d_i \cdot B_i(\Psi_V, P)$$

where d_i are spline coefficients for V and $B_i(\Psi_V,P)$ is the B-spline 'i' for the given set of knots, Ψ_V, at pressure P.

The knots for the B-splines representing V up to 300 mb are the logarithms of $\Psi_V = \{4{*}300,400,500,600,700,850,4{*}1000\}$.

We may represent ΔT and ΔV with B-splines in the same way, with the spline coefficients $\Delta\underset{\sim}{C}$ and $\Delta\underset{\sim}{D}$ respectively. Then (1)-(5) together with the new basis functions will give the linear system

$$\underset{\approx}{R}_T \cdot \underset{\approx}{S} \cdot \Delta\underset{\sim}{C} + \underset{\sim}{R}_S \cdot \Delta T_S + \underset{\approx}{R}_V \cdot \underset{\approx}{U} \cdot \Delta\underset{\sim}{D} = \underset{\sim}{Y} \tag{6}$$

$$\underset{\approx}{A}_T \cdot \Delta\underset{\sim}{C} + \underset{\sim}{A}_S \cdot \Delta T_S + \underset{\approx}{A}_V \cdot \Delta\underset{\sim}{D} = \underset{\sim}{Z} \tag{7}$$

where the new elements in (6) are

$$s_{ij} = \begin{cases} 0 & , \quad i = 1,2,\ldots.10, \; j = 1,\ldots.12, \\ B_j(\Psi_T,P_i) & , \quad i = 11,12,\ldots 40, \; j = 1,\ldots.12, \end{cases}$$

$$u_{ij} = \begin{cases} 0 & , \quad i = 1,2,\ldots.25, \; j = 1,\ldots.9, \\ B_j(\Psi_V,P_i) & , \quad i = 26,27,\ldots.40, j = 1,\ldots.9. \end{cases}$$

Equation (7) is formed by (2)-(5) where

$$\underset{\approx}{A}_T = \begin{pmatrix} 000000000001 \\ 000000000000 \\ 100000000000 \\ 000000000001 \end{pmatrix},$$

$$\underset{\sim}{A}_S = (0,0,0-1)^T ,$$

$$\underset{\approx}{A}_V = \begin{pmatrix} 000000000 \\ 000000001 \\ 000000000 \\ 000000000 \end{pmatrix},$$

$$\underset{\sim}{Z} = (T_{OBS} - t_{40}^{(0)}, V_{OBS} - v_{40}^{(0)}, 0, T_S^{(0)} - t_{40}^{(0)})^T .$$

We have a linear least-squares problem with 22 unknown and m+4 equations. Optimization problems, including least-squares problems, are described in Gill et al (1981). The weighted (6) and (7) can in short form be written

$$\min_{\underset{\sim}{F}}\{||\underset{\approx}{K}\cdot\underset{\sim}{F} - \underset{\sim}{G}||_2\} \tag{8}$$

where

$$\underset{\approx}{K} = \underset{\approx}{E}\cdot\begin{pmatrix} \underset{\approx}{R}_T\cdot\underset{\approx}{S} & \underset{\sim}{R}_S & \underset{\approx}{R}_V\cdot\underset{\approx}{U} \\ \underset{\approx}{A}_T & \underset{\sim}{A}_S & \underset{\approx}{A}_V \end{pmatrix},$$

$$\underset{\sim}{F} = (\Delta\underset{\sim}{C}^T, \Delta T_S, \Delta\underset{\sim}{D}^T)^T ,$$

$$\underset{\sim}{G} = \underset{\approx}{E}\cdot(\underset{\sim}{Y}^T, \underset{\sim}{Z}^T)^T ,$$

$\underset{\approx}{E}$ is a (m+4) x (m+4)-diagonal matrix, where element e_{ii} is the weight for equation 'i'.

This problem is ill-posed. That is, taking the least-squares solution

$$\underset{\sim}{F} = (\underset{\approx}{K}^T \underset{\approx}{K})^{-1} \cdot \underset{\approx}{K}^T \cdot \underset{\sim}{G} ,$$

we will have a physically unacceptable solution, because of the influence of measurement error in the RTE. A survey of inversion problems in remote sensing is found in Twomey (1977). In order to have a physically acceptable and mathematically accurate solution, we may add physical constraints and penalty terms.

2.5 Physical constraints

Physical constraints added to an inverse problem will often, as a complement to other methods, improve the solution. Here we will use two physical constraints, which are transformed to linear inequality constraints.

The dry adiabatic lapse rate, defined in Holton (1979), is constraining the temperature variations by $\frac{dT}{d\ln(P)} \leq R/C_P \cdot T$ where R and C_P are constants. With a representation of T in B-splines we will have in terms of the unknown $\Delta \underset{\sim}{C}$,

$$\sum_{i=1}^{12} (B_i'(\Psi_T,P) - R/C_P \cdot B_i(\Psi_T,P)) \cdot \Delta c_i \leq$$

$$\sum_{i=1}^{12} (-B_i'(\Psi_T,P) + R/C_P \cdot B_i(\Psi_T,P)) \cdot c_i .$$

We check these constraints for the pressure levels 26, 27 ,,,, 40.

The relative humidity has to be in the interval 0 to 100%. The lower limit is automatically fulfilled because we use the variable V = ln(W). From the basic laws of thermodynamics we derive $V \leq \alpha + \beta(1/273 - 1/T)$, where α and β are constants (α depends on the pressure).

This is a nonlinear constraint. We may linearize it by doing a Taylor expansion about $T^{(0)}$ and $V^{(0)}$. In terms of the unknown $\Delta \underset{\sim}{C}$ and $\Delta \underset{\sim}{D}$ we then have

$$\sum_{i=1}^{9} B_i(\Psi_V,P) \cdot \Delta d_i - \beta/(T^{(0)} \cdot T^{(0)}) \cdot \sum_{i=1}^{12} B_i(\Psi_T,P) \cdot \Delta c_i \leq$$

$$\alpha + \beta(1/273 - 1/T^{(0)}) - V^{(0)} .$$

We check these constraints for the pressure levels 26, 27, ..., 40.

2.6 Penalty terms

We will add penalty terms, or regularization functionals, which reflects the supposed behaviour of the solution to the inverse problem. We will require that the variables T and V will be smooth. We then change (8) to

$$\min_{\underset{\sim}{F}} \{||\underset{\approx}{K}\cdot\underset{\sim}{F} - \underset{\sim}{G}||_2 + \lambda_T\cdot I_T + \lambda_V\cdot I_V\} \tag{9}$$

where

$$I_T = \int_{\ln(10)}^{\ln(1000)} (T''(P))^2 d\ln(P) \;,$$

$$I_V = \int_{\ln(300)}^{\ln(1000)} (V''(P))^2 d\ln(P)$$

and λ_T, λ_V are positive, regularization parameters to be decided (T" and V" are short for $\frac{d^2T}{d\ln(P)^2}$ and $\frac{d^2V}{d\ln(P)^2}$. A similar penalty term for temperature profiles, where $(\Delta T)''$ is used instead of T", have been proposed by O'Sullivan and Wahba (1984).

If we use spline representation we will have $I_T = (\underset{\sim}{C} + \Delta\underset{\sim}{C})^T\underset{\approx}{Q}(\underset{\sim}{C} + \Delta\underset{\sim}{C})$ and $I_V = (\underset{\sim}{D} + \Delta\underset{\sim}{D})^T\underset{\approx}{H}(\underset{\sim}{D} + \Delta\underset{\sim}{D})$,

where

$$q_{ij} = \int_{\ln(10)}^{\ln(1000)} B_i''(\Psi_T,P)\cdot B_j''(\Psi_T,P)\cdot d\ln(P) \;, \quad i,\, j \le 12,$$

and

$$h_{ij} = \int_{\ln(300)}^{\ln(1000)} B_i''(\Psi_V,P)\cdot B_j''(\Psi_V,P)\cdot d\ln(P) \;, \quad i,\, j \le 9.$$

The matrices $\underset{\approx}{Q}$ and $\underset{\approx}{H}$ can be calculated analytically with few arithmetic operations. Both matrices are symmetric and positive definite. We make a Cholesky factorization, which gives $\underset{\approx}{Q} = \underset{\approx}{L}_T^T\cdot\underset{\approx}{L}_T$ and $\underset{\approx}{H} = \underset{\approx}{L}_V^T\cdot\underset{\approx}{L}_V$ ($\underset{\approx}{L}_T$ and $\underset{\approx}{L}_V$ are triangular matrices).

Now (9) may be rewritten

$$\min_{\underset{\sim}{F}} (||\underset{\approx}{K}\cdot\underset{\sim}{F}-\underset{\sim}{G}||_2 + \lambda_T||\underset{\approx}{L}_T\cdot\Delta\underset{\sim}{C} + \underset{\approx}{L}_T\cdot\underset{\sim}{C}||_2 + \lambda_V||\underset{\approx}{L}_V\cdot\Delta\underset{\sim}{D} + \underset{\approx}{L}_V\cdot\underset{\sim}{D}||_2), \tag{10}$$

which is an ordinary least-squares problem in the unknown $\Delta \underset{\sim}{C}$, ΔT_S and $\Delta \underset{\sim}{D}$. The regularization parameters λ_T and λ_V have to be estimated. We will do a subjective estimation of the parameters. Several different values of these parameters have been tested and those two, which seemed to give the best result were chosen. The regularization parameters may be automatically computed by the method of generalized cross-validation, see Craven and Wahba (1979) or Golub et al (1979). The algorithms are developed for non-constrained linear, least-squares problems with one regularization parameter. Generalized cross-validation has recently been extended to be used for nonlinear problems by O'Sullivan and Wahba (1984).

2.7 Solving the linear least-squares problems subject to linear inequality constraints

We will now solve the linear least-squares problem (10) subject to the linear inequality constraints described in Section 2.5. We use the algorithm developed by Stoer (1971). This algorithm also solves least-squares problems with equality constraints. If none of the constraints is active, the computational work in solving the problem, is comparable with methods used for linear least-squares problems without constraints.

We have now received a better approximation of $\underset{\sim}{T}$, T_S and $\underset{\sim}{V}$, with $\underset{\sim}{T}^{(1)} = \underset{\sim}{T}^{(0)} + \Delta \underset{\sim}{T}$, $T_S^{(1)} = T_S^{(0)} + \Delta T_S$ and $\underset{\sim}{V}^{(1)} = \underset{\sim}{V}^{(0)} + \Delta \underset{\sim}{V}$. With few modifications of the algorithms, we may use $\underset{\sim}{T}^{(1)}$, $T_S^{(1)}$ and $\underset{\sim}{V}^{(1)}$ as a new initial guess, and repeat the procedure. This will account for the non-linear properties of the radiative transfer equation. Two or three iterations seem to be enough.

3. DATA PROCESSING

The Physical TOVS Export Package, dated 24 September, 1983 and described by Smith et al (1984), was used. The ordinary retrieval program (FXTIRO) was replaced by our method (THAP). The retrieval programs, both FXTIRO and THAP, offer a lot of alternatives. The programs were executed with the following options:

1) Analysed values of surface temperature, surface dewpoint temperature and surface pressure are included.
2) Climate was used as first guess profile.
   In THAP we use another first guess for the water vapour. We use the formula $W(P) = W_{OBS}*(P/P_S)^3$, which is suggested by Smith (1966).
3) Profiles are produced from 3 x 3 arrays of HIRS spots. This will give an approximate horizontal resolution of 75 km.
4) The high-resolution topography with a horizontal resolution of ten nautical miles was used.

In THAP we use the HIRS-channels 3,4,5,6,7,8,10,11,12,13,14,15 and 16 and the MSU-channels 3 and 4. This will give a total of 15 equations derived from the radiative transfer equation. Surface emissivities for the HIRS-channels are given in Table 1, which is taken from Chedin and Scott (1984). Surface emissivity for the MSU-channels is 0.7.

Channel number		7	8	9	10	13	14	18	19
Emissivity	Land	0.98	0.96	0.96	0.93	0.91	0.93	0.88	0.88
	Sea	1.0	0.98	0.98	0.98	0.97	0.98	0.96	0.96

TABLE 1. Surface emissivities for the HIRS channels. An emissivity of 1 is given to the remaining channels.

The weights for the different equations are given in Table 2.

Equation	Weight
Derived from RTE for channel 'ν', eq (6)	$1/\frac{\partial B_\nu(B^{-1}(\gamma_\nu))}{\partial T}$ *
Surface observation of temperature, eq (2)	0.5
Surface observation of humidity, eq (3)	10
Temperature at 10 mb, eq (4)	0.5
Difference between surface temperature and surface skin temperature, eq (5)	0.33

* This weight should be divided with the assumed measurement error in the brightness temperature. According to Susskind and Chahine (1984) this error is estimated to 0.7°K for clear retrievals and 1°K for partly cloudy retrievals. We assume an error of 1°K.

TABLE 2. Weights for each equation used in the inversion method THAP

The regularization parameters were; $\lambda_T = 0.03$ and $\lambda_V = 0.06$. Three iterations were done for each sounding.

4. TESTS

Test data are taken from the Meso-scale Analysis Area for PROMIS 600 at SMHI, see Gustafsson and Törnevik (1984), during the period May 3-26, 1983. Fifteen satellite passages were processed. This area, with the radiosonde stations marked off, is shown in Fig. 1. Temperature retrievals from these radiosondes were compared with satellite soundings in the following way.

1) Radiosonde observations at 00Z and 12Z were used. The nearest time to the satellite passage was used. The radiosonde data have passed certain gross quality checks.
2) The nearest satellite sounding to each radiosonde was chosen. Distance should be less than 150 km.
3) Layer mean temperatures for eight levels were calculated and compared. Root-mean-square difference (RMS), standard deviation (STD) and mean difference (MEAN) were calculated.

Only clear retrievals were analyzed, because the cloud correction algorithms in this version of TOVS Export Package, was not well adapted for our kind of inversion method. Later versions of TOVS Export Package use more suitable cloud correction algorithms. The results from FXTIRO are shown in Fig. 2, while the results from THAP are shown in Fig. 3.

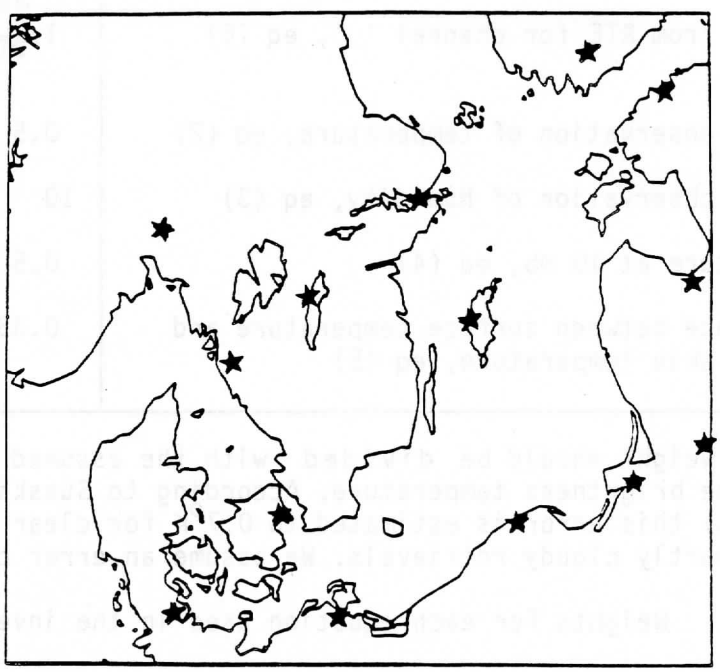

Figure 1. Radiosonde stations in the Meso-scale Analysis Area (appr. 54-61^{o}N, 6-28^{o}E)

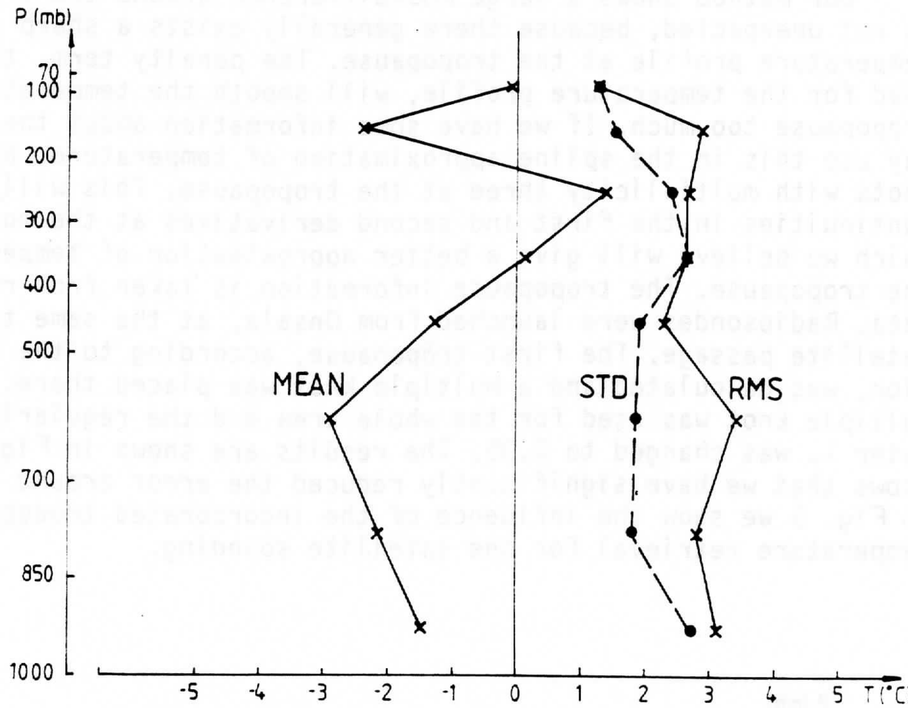

Figure 2. Differences in layer mean temperature between satellite soundings from FXTIRO and radiosondes, launched in the Meso-scale Analysis Area. 104 clear retrievals are included.

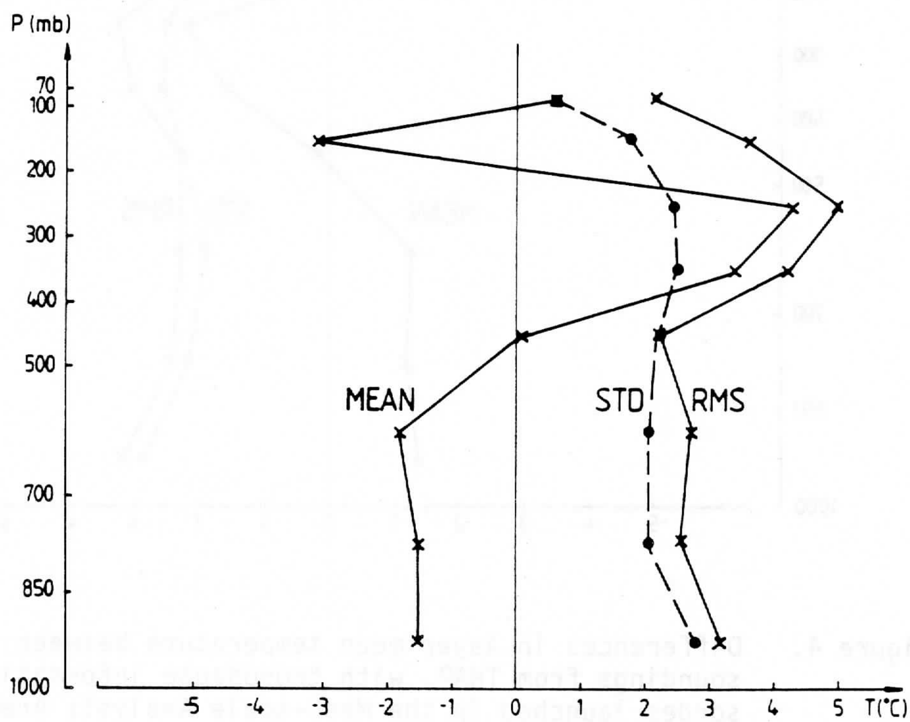

Figure 3. Differences in layer mean temperature between satellite soundings from THAP, without tropopause information, and radiosondes launched in the Meso-scale Analysis Area. 118 clear retrievals are included.

Our method shows a large RMS-difference around the tropopause. This is not unexpected, because there generally exists a sharp edge in the temperature profile at the tropopause. The penalty term, that we have used for the temperature profile, will smooth the temperature around the tropopause too much. If we have some information about the tropopause we may use this in the spline approximation of temperature, by placing knots with multiplicity three at the tropopause. This will give discontinuities in the first and second derivatives at the multiple knot, which we believe will give a better approximation of temperature around the tropopause. The tropopause information is taken from radiosonde data. Radiosondes were launched from Onsala, at the same time as the satellite passage. The first tropopause, according to the WMO definition, was calculated and a multiple knot was placed there. The same multiple knot was used for the whole area and the regularization parameter λ_T was changed to 0.05. The results are shown in Fig. 4. This shows that we have significantly reduced the error around the tropopause. In Fig. 5 we show the influence of the incorporated tropopause on the temperature retrieval for one satellite sounding.

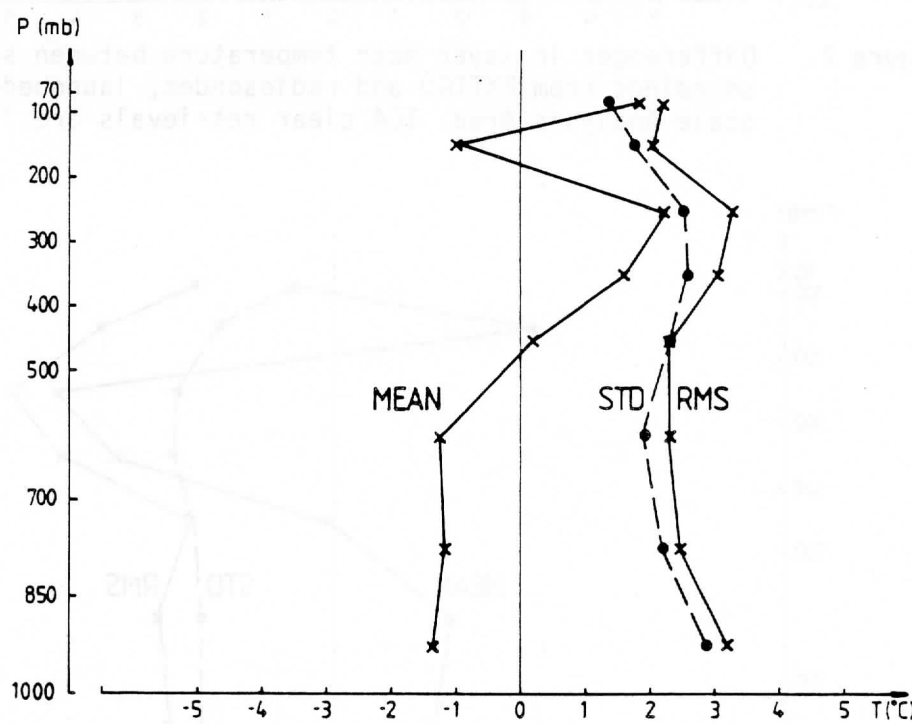

Figure 4. Differences in layer mean temperature between satellite soundings from THAP, with tropopause information, and radiosondes launched in the Meso-scale Analysis Area. 118 clear retrievals are included.

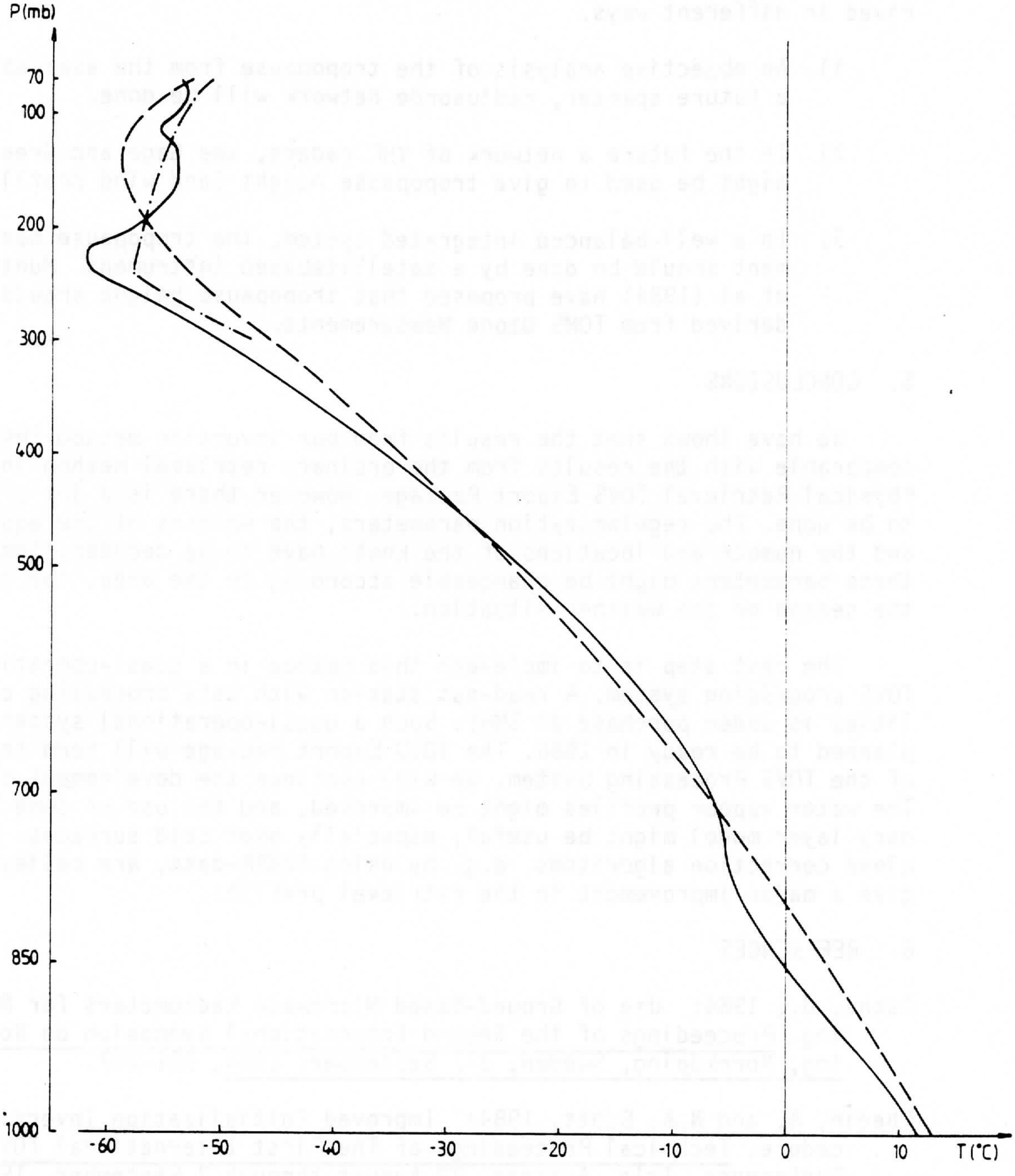

Figure 5. Temperature retrieval from one satellite sounding (1983-05-06 1345, 57°N, 12°E)

——— = radiosonde
------ = THAP, without tropopause
—.— = THAP, with tropopause (temperature below 300 mb will coincide with the retrieval, without tropopause information)

In an operational system, the tropopause information might be derived in different ways.

1) An objective analysis of the tropopause from the available, or a future sparser, radiosonde network will be done.

2) In the future a network of VHF radars, see Gage and Green (1982) might be used to give tropopause height (and wind profiles).

3) In a well-balanced integrated system, the tropopause measurement should be done by a satellitebased instrument. Munteanu et al (1984) have proposed that tropopause height should be derived from TOMS Ozone Measurements.

5. CONCLUSIONS

We have shown that the results from our inversion method THAP are comparable with the results from the ordinary retrieval method in the Physical Retrieval TOVS Export Package. However there is a lot of tuning to be done. The regularization parameters, the weights of the equations and the number and locations of the knots have to be decided. Some of these parameters might be changeable according to the area, the time of the season or the weather situation.

The next step is to implement this method in a quasi-operational TOVS processing system. A read-out station with data processing capabilities is under purchase at SMHI. Such a quasi-operational system is planned to be ready in 1986. The TOVS Export Package will form the base of the TOVS Processing System. We will continue the development of THAP. The water vapour profiles might be improved, and the use of some boundary layer model might be useful, especially over cold surfaces. Better cloud correction algorithms, e.g. by using AVHRR-data, are believed to give a major improvement in the retrieval profiles.

6. REFERENCES

Askne, J., 1984: Use of Ground-Based Microwave Radiometers for Nowcasting. Proceedings of the Second International Symposium on Nowcasting, Norrköping, Sweden, 3-7 September, 1984, 201-207.

Chedin, A. and N.A. Scott, 1984: Improved Initialization Inversion Procedure. Technical Proceedings of The First International TOVS Study Conference, Igls, Austria, 29 August through 2 September, 1983, 14-79.

Craven, P. and C. Wahba, 1979: Smoothing noisy data with spline functions: estimating the correct degree of smoothing by the method of generalized cross-validation. Numerische Mathematik, 31, 377-403.

de Boor, C., 1978: A Practical Guide to Splines. Springer Verlag, New York.

Gage, K.S. and J.L. Green, 1982: An Objective Method for the Determination of Tropopause Height from VHF Radar Observations. Journal of Applied Meteorology, 21, 1150-1154.

Gill, P.E., W. Murray and M.H. Wright, 1981: Practical Optimization, Academic Press, London.

Golub, G., M. Heath and G. Wahba, 1979: Generalized cross validation as a method for choosing a good ridge parameter. Technometrics, 21, 215-223.

Gustafsson, N. and H. Törnevik, 1984: Development of an Operational System for Very-Short-Range Forecasting (VSRF) at SMHI. Proceedings of the Second International Symposium on Nowcasting, Norrköping, Sweden, 3-7 September, 1984, 473-477.

Holton, J.R., 1979: An Introduction to Dynamic Meteorology, Academic Press, New York.

Lauritsen, L., G.J. Nelson and F.W. Porto, 1979: Data extraction and calibration of TIROS-N/NOAA radiometers. NOAA Technical Memorandum NESS 107. U.S. Department of Commerce, National Oceanic and Atmospheric Administration, National Earth Satellite Service, Washington D.C., 73 pp.

Munteanu, M.J., E.R. Westwater and N.C. Grody, 1984: Improvement of MSU Temperature Retrievals by Use of Tropopause Heights Derived from TOMS Ozone Measurements. Technical Proceedings of The First International TOVS Study Conference, Igls, Austria, 29 August through 2 September, 1983, 165-172.

O'Sullivan, F. and G. Wahba, 1984: A cross validated bayesian retrieval algorithm for non-linear remote sensing experiments. Technical Report No 747, Dept of statistics, University of Wisconsin, Madison, Wisconsin, 20 pp.

Smith, W.L., 1966: Note on the Relationship between Total Precipitation Water and Surface Dew Point, Journal of Applied Meteorology, 5, 726-727.

Smith, W.L. and H.M. Woolf, 1976: The use of eigenvectors of statistical covariance matrices for interpreting satellite sounding radiometer observations. Journal of Atmospheric Science, 35, 1127-1140.

Smith, W.L., H.M. Woolf, C.M. Hayden, A.J. Schreiner and J.F. Le Marshall, 1984: The Physical Retrieval TOVS Export Package. Technical Proceedings of The First International TOVS Study Conference, Igls, Austria, 29 August through 2 September, 1983, 227-278.

Stoer, J., 1971: On the numerical solution of constrained least-squares problems. SIAM Journal of Numerical Analysis, 8, 382-411.

Susskind, J. and M.T. Chahine, 1984: The GLAS Physical Numerical Algorithm for Analysis of HIRS 2/MSU Data. Technical Proceedings of The First International TOVS Study Conference, Igls, Austria, 29 August through 2 September, 1983, 285-299.

Svensson, J., 1984: Temperature profile retrievals from TIROS Operational Vertical Sounder during the ONSAM-experiment. R & D notes 33, SMHI, Norrköping, Sweden, 13 pp.

Svensson, J., 1985: Remote sensing of atmospheric temperature profiles by TIROS Operational Vertical Sounder, RMK 45, SMHI, Norrköping, Sweden, (to appear).

Twomey, S., 1977: An introduction to the mathematics of inversion in remote sensing and indirect measurements. Elsevier, New York.

Weinreb, M.P., H.E. Fleming, L.M. McMillin and A.C. Neundorffer, 1981: Transmittances for the TIROS Operational Vertical Sounder, NOAA Technical Report NESS 85, U.S. Department of Commerce, National Oceanic and Atmospheric Administration, National Earth Satellite Service, Washington D.C., 65 pp.

Werbowetski, A. (Ed.), 1981: Atmospheric Sounding User's Guide. NOAA Technical Report NESS 83, U.S. Department of Commerce, National Oceanic and Atmospheric Administration, National Earth Satellite Service, Washington D.C., 82 pp.

The Technical Proceedings of
The Second International TOVS Study Conference

Igls, Austria

February 18 - 22, 1985

Edited by

W. P. Menzel

Cooperative Institute for Meteorological Satellite Studies
Space Science and Engineering Center
University of Wisconsin
1225 West Dayton Street
Madison, Wisconsin 53706
(608)262-0544

September 1985